Case Studies in Thermal Engineering 8 (2016) 1–9

Contents lists available at ScienceDirect

Case Studies in Thermal Engineering

journal homepage: www.elsevier.com/locate/csite

Experimental investigation on the flow behaviour in a bubble pump of diffusion absorption refrigeration systems

Ali Benhmidene [a,*], Khaoula Hidouri [a], Béchir Chaouachi [a], Slimane Gabsi [a], Mahmoud Bourouis [b]

[a] URECAP, Ecole Nationale d'Ingénieurs de Gabès, Route Mednine, 6029 Tunisie
[b] Department of Mechanical Engineering – Universitat Rovira i Virgili, Av. Països Catalans No. 26, 43007 Tarragona, Spain

ARTICLE INFO

Article history:
Received 12 January 2016
Received in revised form
24 March 2016
Accepted 8 April 2016
Available online 9 April 2016

Keywords:
Diffusion absorption refrigeration
Bubble pump
Flow pattern
Oscillation flow

ABSTRACT

An experimental investigation on the performance of a bubble pump for diffusion absorption refrigeration (DAR) systems was carried-out. The characteristics and operating conditions of the bubble pump determine the efficiency of the DAR systems. An experimental set-up operating in continuous mode was designed, built-up and successfully operated as a bubble pump. Experiments were performed by changing some of the parameters affecting the bubble pump performance. The experimental results showed that the performance of the bubble pump was mainly dependent on the driving heat input and the submersion ratio. Driving heat inputs applied were between 20 W and 200 W for a suitable size of the pump tubes. Three submersion ratios were tested, namely 25%, 35% and 45%. The results obtained showed that an oscillating flow was present in the operation of the bubble pump and the frequency of oscillation increased with the increase of the submersion ratio. The average mass flow rate of the refrigerant (ammonia) pumped increased with increase in the heating power; however, mass flow rates of the poor and rich solutions were function of the flow regime. In addition, experimental results were used to determine the optimal heating power for the different submersion ratios considered in this study. The optimal heating power ranged from 30 W to 130 W for a submersion ratio of 25% and from 30 W to 80 W for the submersion ratios of 35% and 45%.

1. Introduction

In diffusion absorption refrigeration (DAR) systems, a thermally driven bubble pump is used to circulate the solution from the absorber to the generator. A bubble pump is simply a vertical tube in which liquid and vapour streams coming from the boiler or generator are introduced at the bottom. The liquid phase fills the lift tube to a predefined height. The vapour phase circulates upwards through this section and forms bubbles that act like pistons driving up the liquid in the remainder section of the tube. The bubble pump is a key component in diffusion absorption refrigeration systems.

Benhmidene et al. [1] reviewed bubble pump configurations from the heating mode point of view. The first configuration reported by the authors is a single lifting tube where the heat input is restricted to a small heating zone at the bottom.

* Corresponding author.
E-mail address: ali.benhmidene@gmail.com (A. Benhmidene).

http://dx.doi.org/10.1016/j.csite.2016.04.002
2214-157X/

Another configuration consists of various lifting tubes, integrated with a flat plate solar collector or indirectly heated bya heat exchanger.

Zohar et al. [2] carried out a thermodynamic analysis to study the effect of three different configurations of the generator and bubble pump on the performance of DAR systems. They concluded that the configuration integrating both the generator and the bubble pump was of great interest.

Two-fluid model was employed by Benhmidene et al. [3,4] to investigate the influence of heat input on a uniformly heated bubble pump at different operating conditions. The optimum heat input was correlated as a function of the tube diameter and mass flow rate, whilst the minimum heat input required for pumping the liquid was correlated as a function of the tube diameter. In addition, Benhmidene et al. [5] investigated the influence of the geometry parameters and operating conditions such as tube diameter, pressure, and ammonia mass fraction in the solution at the bubble pump entrance on the flow parameters at the bubble pump exit. The authors concluded that tube diameter is the parameter that most influences the bubble pump operation.

Ma et al. [6] used the two-fluid model to describe the two-phase flow and heat transfer process in a two-phase closed thermosyphon. They reported that flow patterns predicted numerically and distribution of parameters under different operating conditions showed a good agreement with experimental results.

The uniformly heated tube configuration of the bubble pump was numerically investigated by Garma et al. [7] using the commercial CFD (Computational Fluid Dynamics) tool ANSYS/FLUENT. The effect of heating distribution on the boiling flow of water in a vertical tube showed that the void fraction was higher when the wall was partially heated. Flow regimes repartitions were identified based on the void fraction variation along the tube.

Soo et al. [8] carried out a multidimensional numerical simulation of the saturated flow boiling heat transfer in bubble pumps of diffusion absorption refrigeration cycles. The bubble pump consisting of a vertical tube was uniformly heated at the outer wall surface along the entire pump length. The authors concluded that their numerical model predicted more realistically the performance of ammonia/water bubble pumps than the one-dimensional model.

Pfaff et al. [9] studied the bubble pump for a water/lithium bromide absorption cooling cycle. They developed a mathematical model using the manometer principle to evaluate the bubble pump performance. They reported that the pumping ratio was independent of the heat input. However, the frequency of the pumping action increased when the heat input to the bubble pump was increased, or if the tube diameter was decreased. The model was then used to analyse an ammonia/water bubble pump. The results indicated that the diameter maximizing the efficiency of the bubble pump was between 4 mm and 26 mm for a liquid pumping rate between 0.0025 kg s^{-1} and 0.02 kg s^{-1}. However, the efficiency rapidly decreased when diameters lower than the values of the optimum range were used; therefore they recommended that the diameter should be slightly higher than the values of the optimum range.

Rattnerand Garimella [10] presented an experimental study of a 7.8 mm internal-diameter bubble-pump generator with water-steam as a working fluid over a wide range of operating conditions. This bubble-pump generator could be operated with heat input temperature as low as 11 °C above the fluid saturation temperature. A mechanistic fluid flow and heat transfer model was developed and validated. This investigation demonstrated that integrated fluid-heated bubble-pump

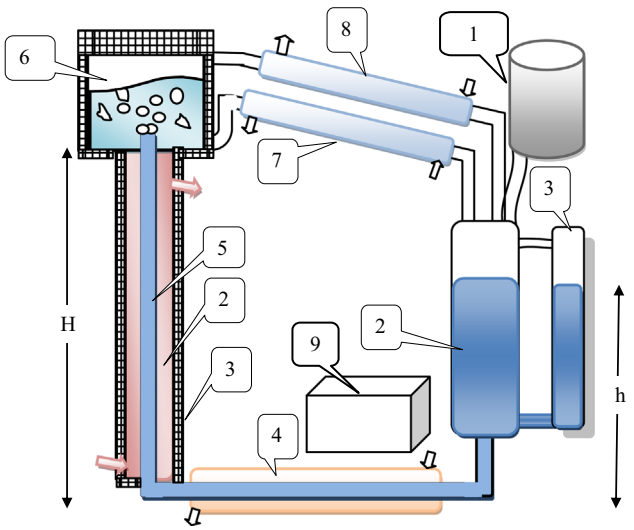

1: Solution preparation tank; 2: Solution reservoir; 3: Level indicator;
4:Heat exchanger; 5: Bubble pump; 6: Separator; 7 Condenser;
8: preheater, 9: Thermostatic bath, 10: heating fluid, 11: insulation

Fig. 1. Technical drawing of the experimental set-up.

generators were a promising alternative to conventional spot-heated configurations and could enable refrigeration using low-grade thermal energy.

Ben Ezzineet al. [11] performed an experimental investigation of an air-cooled diffusion-absorption refrigeration machine. A new concept of generator consisting of separate boiler and bubble pump instead of the usual combined generator was tested. Heat input in the bubble pump was varied from 170 W to 350 W, while the driving temperature was in the range 120–150 °C. The lowest temperature reached at the evaporator entrance was 10 °C for a driving temperature of 138 °C and a heat input of 260 W. The COP (Coefficient of operation) of the machine at these operating conditions reached a maximum of 0.14.

Jakobet al. [12] reported that an indirectly heated generator that incorporated the bubble pump was the main new feature of a solar heat driven ammonia/water diffusion absorption refrigeration machine and that all the prototypes constructed performed well. The maximum COP reached was 0.38.

Other experimental and theoretical studies (Nicklin [13], Lister [14], Jeong et al. [15]) showed that, for a specific heat input, the diameter of the lift tube had no effect on the pumping rate if the pump was running in the slug or churn flow regimes. When the maximum lift-tube diameter is exceeded, the flow pattern changes from slug flow to an intermittent churn-type flow. After exceeding a certain pumping height, the pumping action stopped.

In the present work, a continuous experimental set-up was designed, built-up and successfully operated as a bubble pump with ammonia/water as a working pair. The effect of heat input and submersion ratio on the performance of the heat pump was experimentally investigated.

2. Description of the experimental set-up and procedure

2.1. Experimental set-up

The experimental set-up shown in the technical drawing of Fig. 1, consisted of a solution preparation tank, a solution reservoir, a liquid pre-heater, a bubble pump, a liquid/vapour phase separator, a condenser and a cooling system Ammonia/water was used as a working fluid. Ammonia/water solution, stored in the preparation tank, entered the bubble pump through the reservoir container according to a predefined submersion ratio. Heating was applied along the tube using a heat transfer fluid from a thermostatic bath. The liquid/vapour mixture pumped by the bubble pump was separated in a liquid/vapour separator. The vapour phase was condensed in a water cooled condenser in which the mass flow rate of the condensate was measured at the outlet. Simultaneously, the mass flow rate of the pumped poor solution was measured. The condensate and the poor solution were then mixed in the reservoir container and the mixture was supplied back to the bubble pump through a heat exchanger. The separator and the bubble pump were insulated with glass wool.

2.1.1. Solution preparation tank

Water and ammonia quantities to be used to prepare the charge of the working fluid were calculated according to the desired ammonia mass fraction. The ammonia vapour was introduced slowly into the preparation tank after introducing the desired water quantity. The absorption process of ammonia vapour in water was carried out during several hours and required cooling which was performed by a water stream flowing through a coil mounted in the preparation tank. During the absorption process, pressure prevailing in the tank was controlled.

2.1.2. Liquid pre-heater

The rich solution in ammonia passed through a pre-heater to achieve saturated temperature before entering the bubble pump. The pre-heater was a heat exchanger formed by two coaxial tubes of stainless steel. The rich solution flowed inside the inner tube heated by hot water which circulated in the annular space fed by a thermostatic bath at a fixed temperature of 60 °C.

2.1.3. Bubble pump

The bubble pump consisted of a coaxial double-tube. The rich solution circulated in the inner tube where as the heating fluid flowed in the annulus at a fixed flow rate in all experiments. Heating was provided by a thermostatic bath whose maximum heating power was 3500 W. An insulation layer was attached along the bubble pump tube to minimize heat losses. Bubble pump was charged with the rich solution according to a defined submersion ratio (h/H), where h is the rich solution level in the reservoir and H is its level in the bubble pump.

2.1.4. Liquid/vapour separator

The liquid/vapour mixture was pumped to the separator which is a hollow cylinder of stainless steel, where the poor solution (liquid) and refrigerant vapour were separated.

2.1.5. Condenser

The condenser was made of two coaxial tubes. In the annular space cooling water flowed at a temperature of 26 °C.

2.1.6. Cooler

The cooler was also made of two coaxial tubes with similar dimensions to those of the condenser. The hot poor solution flowed in the inner tube whereas cooling water circulated in the annular space.

Table 1
Summary of the operating conditions considered in the experimental work.

Parameter	Value
Ammonia mass fraction (dimentionless)	0.6
Submersion ratio (%)	25, 35, 45
Tube diameter of the bubble pump (mm)	6
Tube length of the bubble pump (m)	1.6
Heat input (W)	20–200

2.1.7. Reservoir

The condensate of ammonia and the subcooled poor solution were mixed in the reservoir. The new ammonia/water rich solution passed to the bubble pump tube through a pre-heater. The mixture in the tank was cooled by water flowing inside a coil along the tank. This reservoir was connected to a level indicator.

2.2. Experimental measurements

For the selected operating conditions and geometrical parameters summarized in Table 1, temperature and pressure at the inlet and outlet of each component were measured and stored at 60 s intervals by a registration system. Mass flow rates of the condensate (ammonia liquid) and poor solution were measured at the inlet of the cooler and condenser, respectively. Therefore, the influence of heat input on the bubble pump performance was investigated. The variation with mass flow of various parameters of the heat pump was analysed at different values of heat input.

Data reduction was based on the following energy and mass balances:

Heat input was calculated according to the flowing expression:

$$\dot{Q} = \dot{m}_r H_r - (\dot{m}_P H_P + \dot{m}_C H_C) \tag{1}$$

Mass flow rate of the rich solution was obtained from the overall mass balance in the reservoir:

$$\dot{m}_r = \dot{m}_P + \dot{m}_C \tag{2}$$

where:

H_r is the enthalpy of the rich solution which was calculated from pressure and temperature at the entrance of the bubble pump.

H_P is the enthalpy of the poor solution which was calculated from pressure and ammonia mass fraction at the exit of the bubble pump.

H_C is the enthalpy of ammonia vapour which was calculated from temperature and pressure prevailing in the separator. It was assumed that there was only ammonia in the vapour phase.

3. Results and analysis

Table 2 shows some registered data including ammonia mass fraction in rich and poor solutions. Ammonia mass fraction was calculated using the property library implemented in the software Engineering Equation Solver (EES).

According to pressure values reported in Table 2, there is hardly a difference between the reservoir and separator pressures. The average value of pressure was around 11 bar. Minimum driving temperature at the entrance of the bubble pump was about 60 °C while the maximum driving temperature was 68 °C. The minimum ammonia mass fraction in the poor solution was in the range 0.41–0.50 at different values used for submersion ratio and heat input.

Table 2
Registered and calculated parameters.

	Submersion ratio		
Variables	45%	35%	25%
$P_{Separator}$ (bar)	11.4–12.5	10.1–12.3	10–11.5
$P_{Reservoir}$ (bar)	11.2–12.5	10–11	9.7–11.3
$T_{Separator}$ (°C)	60–71	62–74	70–82
$T_{Bubble\ pump\ entrance}$ (°C)	59–62	60–61	60–68
Heat input (W)	20–125	21.8–145	22–200
$T_{Cooling\ water}$ (°C)	25–27	25–27	25–27
X_r	0.6	0.6	0.6
X_P	0.55–0.5	0.51–0.48	0.46–0.41

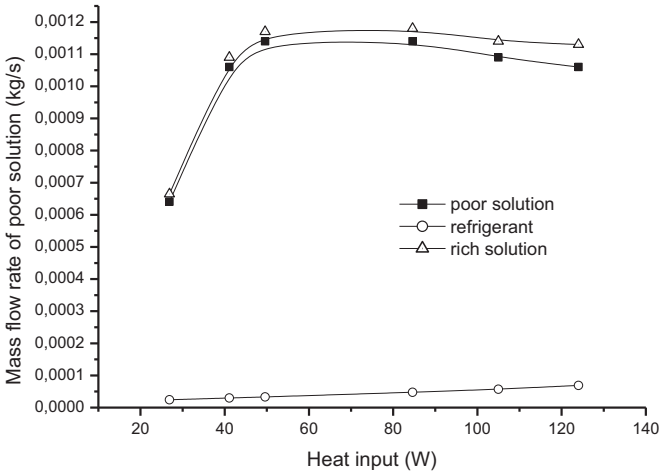

Fig. 2. Variation of refrigerant, poor and strong solution mass flow rates versus heat input.

3.1. Flow patterns in the bubble pump

Fig. 2 shows the mass flow rate variation versus heat input for the refrigerant (ammonia) and rich and poor solutions. A linear variation of the mass flow rate of refrigerant was obtained when heat input was increased, whereas the poor and rich solution mass flow rates sharply increased to achieve a maximum value and then decreased as heat input was increased. Similar results were reported by other investigations in the literature (Jeong et al. [16], Benhmidene et al. [15]). This trend of poor and rich solution mass flow rates versus heat input was due to the flow regime transition. For low values of heat input (under 30 W) and a submersion ratio of 45%, the flow pattern in the bubble pump was the bubbly flow regime, which was oscillating. When the bubble pump received more heat, the vapour generation increased leading to a slug flow, in which the vapour phase was able to raise the liquid phase in the bubble pump (increase of mass flow rate). Then, churn flow regime started at higher values of heat input resulting in an increase of the mass flow of the pumped solution.

Fig. 3 shows how the refrigerant mass flow rate increased linearly with heat input for all values considered for the submersion ratio. This could be explained by an increase in the vapour generation rather than the increase of the solution level. The refrigerant mass flow rate also increased with the submersion ratio as the volume of the heated solution in the bubble pump was higher.

Fig. 4 illustrates that mass flow rate of the poor solution had similar trend versus heat input at different values of the submersion ratio; however, the heat input corresponding to the maximum mass flow rate decreased as the submersion ratio was increased.

The results allow us to establish the heat input required for each flow pattern. The optimal heat input for the bubble pump operation corresponds to slug flow regime (Delano [17], Zuber and Findlay [18]). The average value of the optimal heat input was 80 W for submersion ratios of 35% and 45% and increased to 130 W for the submersion ratio of 25%. On the

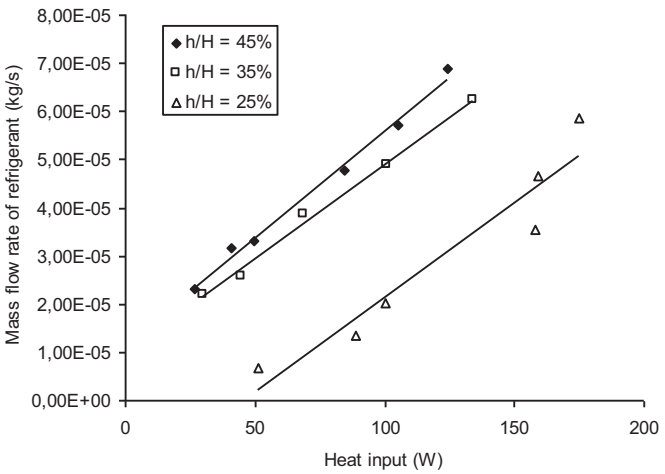

Fig. 3. Refrigerant mass flow rate versus heat input at different values of the submersion ratio.

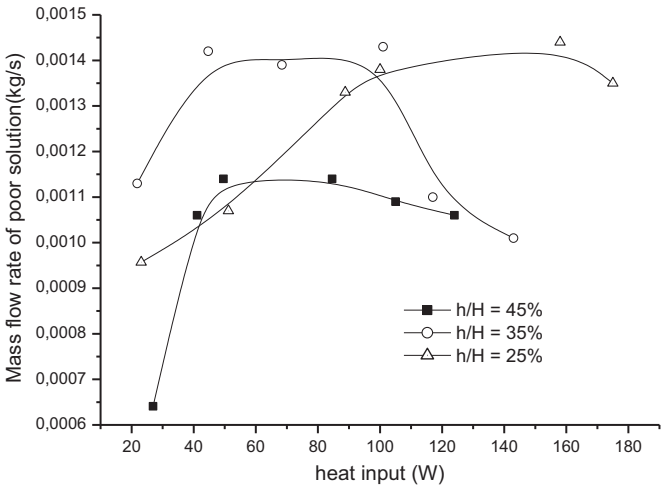

Fig. 4. Refrigerant mass flow rate versus heat input at different values of the submersion ratio.

bases of these result we reported in Table 3 the different values of heat inputs for the flow regimes detected at different values of the submersion ratio.

3.2. Flow stability in the bubble pump

3.2.1. Flow regime visualization

The bubble pump was tested for three submersion ratios and ammonia mass fraction of 0.6. The flow pattern of the liquid-vapour mixture in the bubble pump was visualized using a transparent quartz tube of 6 mm diameter. For low values of heat input (less than 30 W), the solution oscillated inside the pump tube without being lifted up. This was due to the insufficient amount of vapour needed to raise the solution to the separator. Increasing the heating power increased the amount of refrigerant vapour generated. The pumping action was then achieved but was discontinuous. The time interval between two consecutive pumping actions was not constant and decreased with the increase of heating power.

3.2.2. Pressure oscillation

In order to analyse the flow stability in the bubble pump, pressure in the separator is plotted versus time in Fig. 5(a), (b) and (c) at submersion ratios of 25%, 35% and 45%, respectively. Heat input was set at 90 W. As shown in these figures, an aperiodic oscillating flow was observed versus time which confirmed the pumping instability along the bubble pump. Moreover, the frequency of oscillation increased with the increase of the submersion ratio.

Fig. 6(a), (b) and (c) depict the pressure prevailing in the separator and the reservoir at different values of the submersion ratio. It can be seen that the pressure difference between the two components was very small for the submersion ratio of 25% and increased for the submersion ratios of 35% and 45% due to the increase of pressure drop with the submersion ratio.

4. Conclusions

An experimental set-up was built-up to test the performance of an NH_3/H_2O bubble pump of 1.6 m length and 6 mm inner tube diameter. The aqueous solution of ammonia was heated by a heat transfer fluid flowing in the annular space. Driving heat input was in the range of 20–200 W and the average cooling water temperature was 26 °C.

Pressure and temperature at different points of the set-up were registered and stored by a data acquisition system. The experimental data showed the oscillation of pressure at different values of the submersion ratio. Pressures prevailing in the separator and the reservoir were similar at a submersion ration of 25% and increased for the submersion ratios of 35%

Table 3
Heat inputs for the flow regimes detected at different values of the submersion ratio.

	Flow regime			
	Submersion ratio (%)	**Bubbly**	**Slug**	**Churn + annular**
Heat input (W)	25	< 30	30–150	> 150
	35	< 30	30–80	> 80
	45	< 30	30–80	> 80

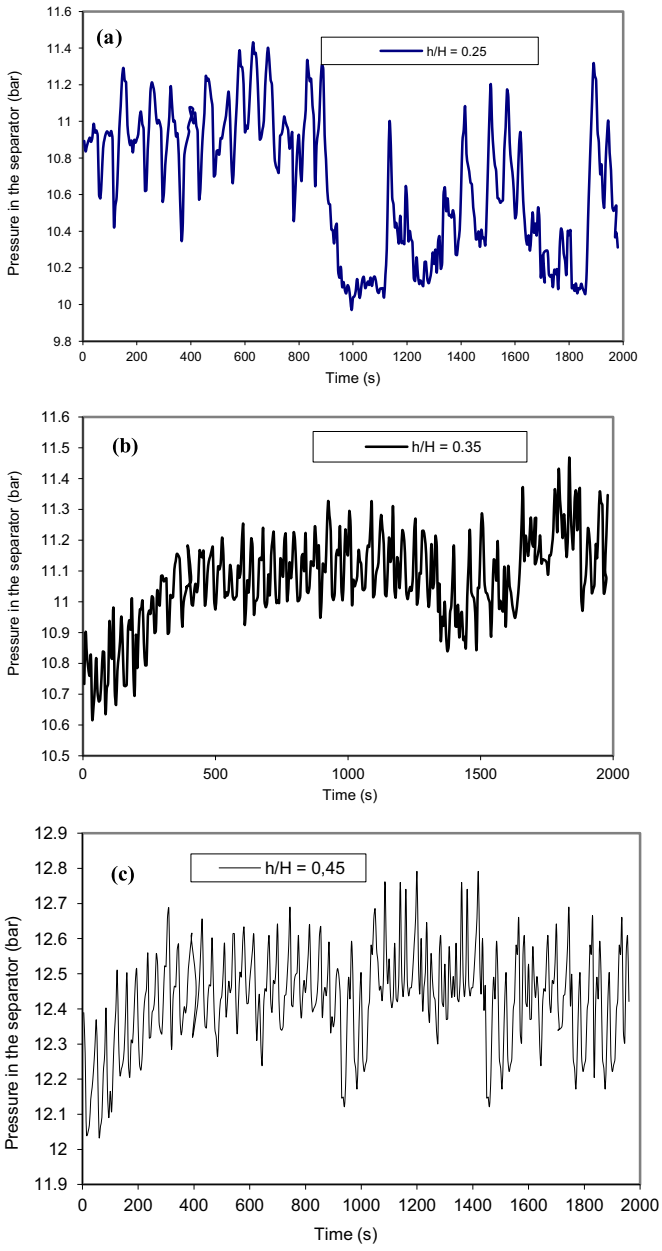

Fig. 5. Variation of the separator pressure versus time at different values of the submersion ratio.

and 45%.

The average mass flow rate of the refrigerant (ammonia) increased linearly by increasing the heating power, whereas the poor and rich solution mass flow rates increase to achieve a maximum value and then decreased as heat input was increased due to the transition of flow regime. Experimental data of the mass flow rate of the poor solution was used to establish the optimal heating power for different values of the submersion ratio. This optimal heating power ranged from 30 W to 130 W for a submersion ratio of 25% and from 30 W to 80 W for the submersion ratios of 35% and 45%.

Acknowledgements

This work is part of a R&D project funded by the Spanish Ministry of Science and Innovation within the Energy Program: ENE2006-15250, and is also partly supported by the AECID-PCI Spanish Tunisian cooperation program: AP/037031/11.

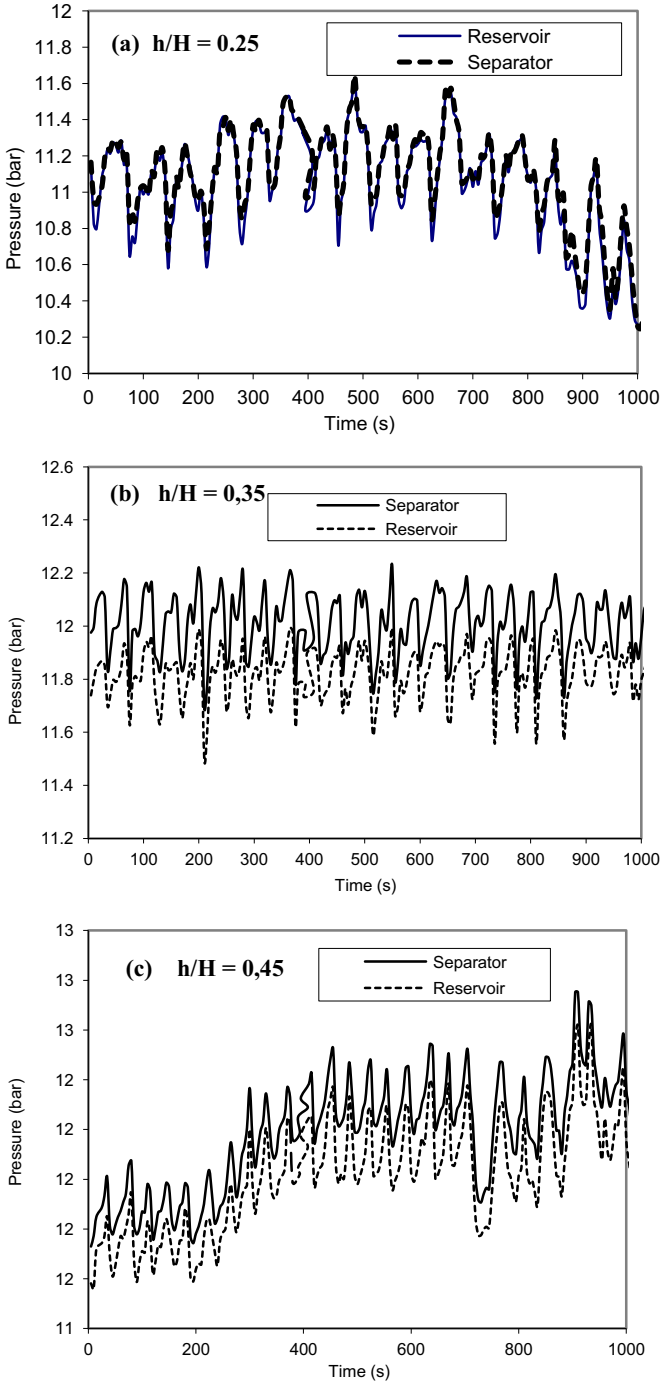

Fig. 6. Pressure prevailing in the separator and the reservoir at different values of the submersion ratio.

References

[1] A. Benhmidene, B. Chaouachi, S. Gabsi, A review of bubble pump technologies, J. Appl. Sci. 10 (2010) 1806–1813.
[2] A. Zohar, M. Jelinek, A. Levy, I. Borde, The influence of the generator and bubble pump configuration on the performance of diffusion absorption refrigeration (DAR)system, Int. J. Refrig. 31 (2008) 962–969.
[3] A. Benhmidene, B. Chaouachi, S. Gabsi, M. Bourouis, Modelling of the heat flux received by a bubble pump of absorption-diffusion refrigeration cycles, Heat. Mass Transf. 47 (2011) 1341–1347.
[4] A. Benhmidene, B. Chaouachi, S. Gabsi, M. Bourouis, Modelling of boiling two-phase flow in the bubble pump of diffusion absorption refrigeration, Chem. Eng. Commun. 202 (2015) 15–24.

[5] A. Benhmidene, B. Chaouachi, M. Bourouis, S. Gabsi, Effect of operating conditions on the performance of the bubble pump of absorption-diffusion refrigeration cycles, Therm. Sci. 15 (2011) 793–806.
[6] Zh. Ma, A. Turan, Sh. Guo, Practical numerical simulations of two-phase flow and heat transfer phenomena in a thermosyphon for design and development, ICCS, Part I, 2009, pp. 665–674.
[7] R. Garma, Y. Stiriba, M. Bourouis, A. Bellagi, Numerical investigations of the heating distribution effect on the boiling flow in the bubble pumps, Int. J. Hydogen Energy 39 (2014) 15256–15260.
[8] S.W. JO, S.A. Sherif, W.E. Lear, Numerical simulation of saturated flow boiling heat transfer of ammonia/water mixture in bubble pumps for absorption–diffusion refrigerators, ASM J. Therm. Sci. Eng. Appl. 6 (2013).
[9] M. Pfaff, R. Saravanan, M.P. Maiya, S.S. Murthy, Studies on bubble pump for water–lithium bromide vapour absorption refrigeration, Int. J. Refrig. 21 (1998) 452–462.
[10] A.S. Rattner, S. Garimella, Coupling-fluid heated bubble pump generators: Experiments and model development, Sc. Tech. Built Environ. 21 (2015) 332–347.
[11] N. Ben Ezzine, R. Garma, M. Bourouis, A. Bellagi, Experimental studies on bubble pump operated diffusion absorption machine based on light hydrocarbons for solar cooling, Renew. Energy 35 (2010) 464–470.
[12] U. Jakob, U. Eicker, D. Schneider, M.J. Cook, A.H. Taki, Simulation and experimental investigation into diffusion absorption cooling machines for air-conditioning applications, Appl. Therm. Eng. 28 (2008) 1138–1150.
[13] D.J. Nicklin, The air-lift pump: theory and optimization, Trans Inst. Chem. Eng. 41 (1963) 29–38.
[14] G.D.S. Lister, The Design and Evaluation of a Pumping System for a Three Fluid Absorption Refrigeration Plant (B.Sc. thesis), University of Cape Town, Cape Town, South Africa, 1996.
[15] S. Jeong, S.K. Lee, K.K. Koo, Pumping characteristics of a thermosyphon applied for absorption refrigerators with working pair of Li/Br, Appl. Therm. Eng. 18 (1998) 1309–1323.
[16] A. Benhmidene, B. Chaouachi, M. Bourouis, S. Gabsi, Numerical prediction of flow patterns in the bubble pump, ASM J. Fluids Eng. 133 (2011) 031302–031309.
[17] A.D. Delano, Design Analysis of the Einstein Refrigeration Cycle (Ph.D. Dissertation), Georgia Institute of Technology, 1998.
[18] N. Zuber, J. Findlay, Average volumetric concentration in two-phase flow systems, J. Heat. Transf. 87 (1965) 453–468.